

Nanobiocatalysts

International Edition: DOI: 10.1002/anie.201600590
German Edition: DOI: 10.1002/ange.201600590

Enzyme Shielding in an Enzyme-thin and Soft Organosilica Layer

M. Rita Correro, Negar Moridi, Hansjörg Schützinger, Sabine Sykora, Erik M. Ammann, E. Henrik Peters, Yves Dudal, Philippe F.-X. Corvini, and Patrick Shahgaldian*

Abstract: The fragile nature of most enzymes is a major hindrance to their use in industrial processes. Herein, we describe a synthetic chemical strategy to produce hybrid organic/inorganic nanobiocatalysts; it exploits the self-assembly of silane building blocks at the surface of enzymes to grow an organosilica layer, of controlled thickness, that fully shields the enzyme. Remarkably, the enzyme triggers a rearrangement of this organosilica layer into a significantly soft structure. We demonstrate that this change in stiffness correlates with the biocatalytic turnover rate, and that the organosilica layer shields the enzyme in a soft environment with a markedly enhanced resistance to denaturing stresses.

Biocatalysis is a major driver of the chemical industry.^[1] However, the use of enzymes in industrial processes is limited by their significant fragility and fast aging in nonphysiological environments. In addition to genetic engineering techniques to improve enzyme stability,^[2] a variety of chemical approaches have been developed to immobilize and shield enzymes on solid carriers.^[3] Enzyme immobilization on solid supports is a valuable approach to address enzyme stability, and has the additional benefit of allowing the biocatalyst to be retained for continuous operations.

A large number of bioconjugation strategies have been developed to enable the immobilization and protection of enzymes on a variety of carrier materials,^[4] such as (bio-)polymers, zeolites, noble metals, and metal or metalloid oxides (e.g., silica). Recently, sophisticated approaches, in which enzymes were confined and protected in materials, such as metal-organic frameworks^[5] or virus-like particles,^[6] have been developed.

Silica is a material of choice for the immobilization and protection of enzymes, as it has the advantages of low production cost and high thermal and mechanical stability. Sol-gel methods have been extensively developed to embed

enzymes in silica matrices.^[7] Reetz et al. reported the entrapment of a lipase in chemically modified silica gels. The enzyme was immobilized in a sol-gel matrix containing mixtures of tetramethyl orthosilicate and alkyl silanes. A strong dependence of the silane composition of the matrix on the enzymatic activity was demonstrated.^[7c,d] However, the main focus of sol-gel methods to protect enzymes has been on macroscopic systems that do not allow control of the three-dimensional structure of the material produced. Consequently, most techniques are not amenable to the production of discrete functional nanoparticles that can be dispersed into fluids, hence severely limiting their use in biomedical applications. Additionally, silica is inherently negatively charged and can not create a shell closely surrounding the whole surface of the protein. We expected that the presence in these silica-based materials of additional functional groups would increase the number of interaction points with the protein surface and should allow for better protection of the enzyme, owing to better chemical complementarity between the surface of the enzyme and the protective material. Furthermore, the environment shielding the enzyme should be designed in such a way that it does not hinder the conformational dynamic mobility of the enzyme, which is crucial for its biocatalytic activity.^[8] This issue has been often neglected in the design of enzyme-protection systems.

We recently demonstrated that a virus can serve as a template for the growth of an organosilica layer on its capsid surface under purely aqueous conditions.^[9] Herein, we report a synthetic strategy to grow a protective layer of controlled thickness at the surface of immobilized enzymes. The method consists of a sequential reaction involving immobilization of an enzyme on the surface of silica particles, and controlled self-assembly and subsequent polycondensation of silanes, thus resulting in the growth of an organosilica layer on the surface of the particles (Figure 1).

As the carrier material, we chose amino-modified silica nanoparticles (SNPs), which were produced with a diameter of (266 ± 1) nm, as measured by field-emission scanning electron microscopy (FESEM). The amine groups enabled the further covalent anchoring of the target enzyme, β -galactosidase (β -gal) from *Kluyveromyces lactis*, by the use of glutaraldehyde as a homobifunctional cross-linker. The

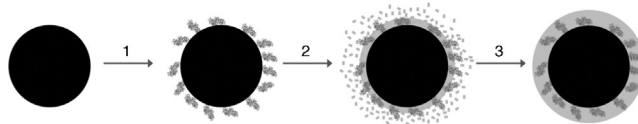


Figure 1. Principle of enzyme protection. Step 1: enzyme immobilization at the surface of SNPs (in black); steps 2 and 3: silane self-assembly and polycondensation.

[*] Dr. M. R. Correro, Dr. N. Moridi, H. Schützinger, S. Sykora, E. M. Ammann, E. H. Peters, Prof. Dr. P. F. X. Corvini, Prof. Dr. P. Shahgaldian
School of Life Science
University of Applied Sciences and Arts Northwestern Switzerland
Gründenstrasse 40, 4132 Muttenz (Switzerland)
E-mail: patrick.shahgaldian@fnw.ch
H. Schützinger, Dr. Y. Dudal
INOFEA AG
Hochbergerstrasse 60C, 4057 Basel (Switzerland)
Prof. Dr. P. F. X. Corvini
School of the Environment, Nanjing University
210093 Nanjing (China)

Supporting information and the ORCID identification number(s) for the author(s) of this article can be found under <http://dx.doi.org/10.1002/anie.201600590>.

enzymatic activity, which was measured by using the conventional *o*-nitrophenyl- β -galactoside (ONPG) assay, showed that less than 1% of the enzyme was left free in the supernatant, a value that was consistent with the total protein concentration, which was under the limit of detection of the method (see the Supporting Information). The enzyme-activity assay showed a loss of 60% of the initial activity. This decrease in activity could be explained by the unfavorable orientation of a fraction of the immobilized enzymes or partial denaturation upon immobilization. The particles were subsequently incubated with a mixture of (3-aminopropyl)-triethoxysilane (APTES, 19 mg mL⁻¹) and tetraethylorthosilicate (TEOS, 80 mg mL⁻¹) to enable the growth of an organosilica layer at the surface of the enzyme. β -Gal from *K. lactis* is a large tetrameric enzyme comprising a dimer of dimers with two biocatalytic centers located at the interface within each dimer.^[10] This three-dimensional structure can be approximated as a triaxial ellipsoid with dimensions of 15.9 \times 9.3 \times 5.3 nm³. Assuming that the immobilization strategy used in the present study did not favor any specific orientation of the protein with regard to the surface, the protective layer would need a thickness of at least 16 nm to fully shield the enzyme. The organosilane polycondensation reaction on the SNPs with surface-immobilized β -gal (SNP_{ENZ-OS}) was monitored over time (Figure 2).

The evolution of the particle diameter over time was found to be linear, with an increase of 1.2 nm h⁻¹. In the last sample collected after polycondensation for 15 h, the thickness of the organosilica layer (17.0 \pm 0.6 nm) was sufficient to

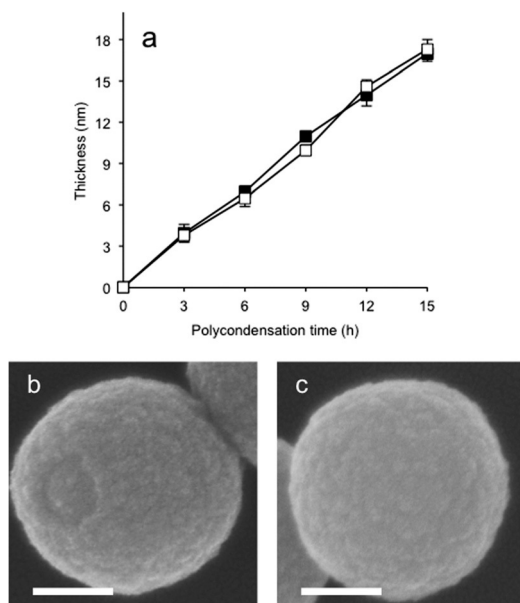


Figure 2. Microscopy study. a) Kinetics of layer growth (mean \pm standard error of the mean) at the surface of SNPs with (SNP_{ENZ-OS}, white squares) or without (SNP_{OS}, black squares) surface-immobilized β -gal, as measured from FESEM images. For both systems, a linear diameter increase of 1.2 nm h⁻¹ was observed, thus showing that the presence of the enzyme at the surface of the SNPs did not significantly influence the kinetics of layer growth. b,c) FESEM images of SNP_{ENZ-OS} with a protective organosilica layer of 17 nm. The particle in (b) has a damaged protective layer; the rounded edge of this layer suggests a soft material. Scale bars represent 100 nm.

shield the whole enzyme, regardless of its orientation to the SNP surface. All particles presented a fairly homogeneous and flat surface. There were only a few sporadic cases in which the layer was partially broken, and its edges did not appear sharp, thus suggesting that this organosilica layer was soft.

When measuring the enzymatic activity of the shielded β -gal (SNP_{ENZ-OS}), we noticed that the enzymatic activity was low for freshly produced SNP_{ENZ-OS} right after synthesis, whereas after storage for 12 h at 25 °C, the same sample had significantly higher activity. Indeed, the activity measured before the layer growth was 73 mU mg⁻¹, which dropped to 21 mU mg⁻¹ after layer growth. After storage for 12 h at 20 °C, the activity was found to be 50 U mg⁻¹, which corresponds to recovery of 68% of the activity of the initially immobilized enzyme. From our experience with virus-imprinted particles, we knew that the organosilica layer was not mechanically stable after the synthesis and had to be stored at room temperature for 12 h to gain stability.^[9a] We decided to investigate this phenomenon further and to assess possible changes in the nanomechanical properties of the protective layer by means of atomic force microscopy (AFM).

The AFM experiments were carried out by measuring force–distance curves on different SNPs of the same sample (Figure 3). As expected, bare SNPs were stiff, with a stiffness value of (34 \pm 0.11) N m⁻¹ (Figure 3). At the beginning of the curing reaction, the SNP_{ENZ-OS} particles were also stiff, with an average value of (14 \pm 0.02) N m⁻¹. After curing for 5 h, the stiffness value dropped to 6 mN m⁻¹ with a moderately broader distribution. The softening effect of the organosilica–protein layer continued until the SNP_{ENZ-OS} reached a value as low as 0.5 mN m⁻¹ after 12 hours, this value then remained constant for several days. By contrast, the SNP_{OS} sample did not exhibit such a trend. The organosilica layer in these reference particles was soft, with a value of 0.28 N m⁻¹ after termination of the layer-growth reaction; this values did not change significantly over the time period of the curing.

The formation of covalent siloxane (Si–O–Si) bonds first requires the hydrolysis of the ethoxy functions of the silanes into the corresponding silanols, which further undergo a condensation reaction. In the present case, one could assume that the initial stiff layer was predominantly stabilized by hydrogen bonds (H-bonds) and ionic interactions of the silanes of short polysiloxanes with the surface of the protein; this layer became softer through the formation of Si–O–Si bonds.

Regarding the change in enzymatic activity, two hypotheses could explain the recovery of enzyme activity during the curing/softening of the organosilica layer. The first is that an increase in porosity of the protective layer resulted in a higher mass transfer of the substrate to the active site of the enzyme. The second hypothesis is that the soft environment of the organosilica layer allowed the protein to acquire sufficient conformational mobility, known to be of crucial importance for the catalytic activity of the enzyme.^[8] To better understand the recovery of enzymatic activity during the curing phase, we performed a kinetic study of the enzymatic activity of freshly produced samples submitted to the curing reaction at 25 °C (Figure 4).

Although the maximum velocity of SNP_{ENZ-OS} increased over curing time, the apparent Michaelis–Menten constant

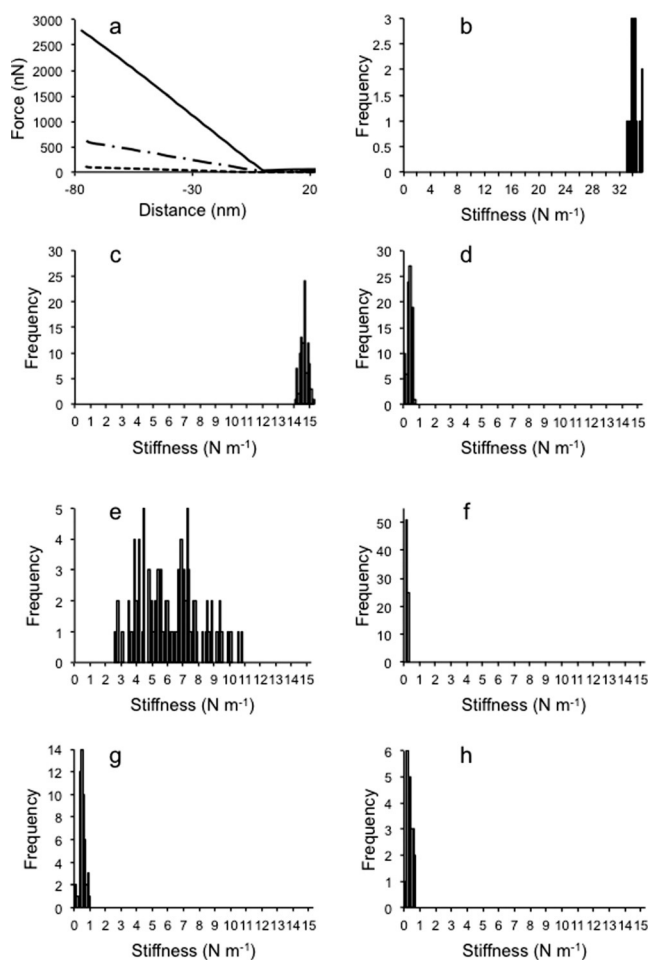


Figure 3. Assessment of nanomechanical properties. a) Force–distance measurements carried out on bare silica nanoparticles (—), SNP_{OS} (----), and $\text{SNP}_{\text{ENZ-OS}}$ (-·-·-) after storage for 12 h. b–h) Stiffness distribution histograms for bare SNPs (b) and $\text{SNP}_{\text{ENZ-OS}}$ (c, e, and g) and SNP_{OS} (d, f, and h) after curing for 2 (c, d), 5 (e, f), and 12 h (g, h).

$K_{\text{m}}^{\text{app}}$ remained relatively unchanged, with values averaging 4 mM, similar to that of the native enzyme (Figure 4). These results allowed us to rule out the possibility that the recovery of enzyme activity was due to an increase in the porosity of the protective organosilica layer. Indeed, in that case, the $K_{\text{m}}^{\text{app}}$ values would have varied, whereas the $V_{\text{m}}^{\text{app}}$ should have remained constant. Therefore, our results provide clear evidence that the recovery of enzyme activity was due to a favorable change in enzyme conformation enabled by the softness of its protective layer.

The recyclability of $\text{SNP}_{\text{ENZ-OS}}$ was tested by repetitive cycles of centrifugation/resuspension in fresh buffer. No relevant loss of activity was measured after 10 cycles. We also applied a series of stress conditions to $\text{SNP}_{\text{ENZ-OS}}$ (Figure 5). The biocatalytic hydrolytic activity of $\text{SNP}_{\text{ENZ-OS}}$, SNP_{ENZ} , and free β -gal were tested at increasing reaction temperatures. The activity of the SNP_{ENZ} and β -gal exhibited a similar trend, with more than 20% activity loss at 45°C, 53% at 50°C, 79% at 55°C, and as much as 96% at 60°C (Figure 5). In contrast, the behavior of $\text{SNP}_{\text{ENZ-OS}}$ was very

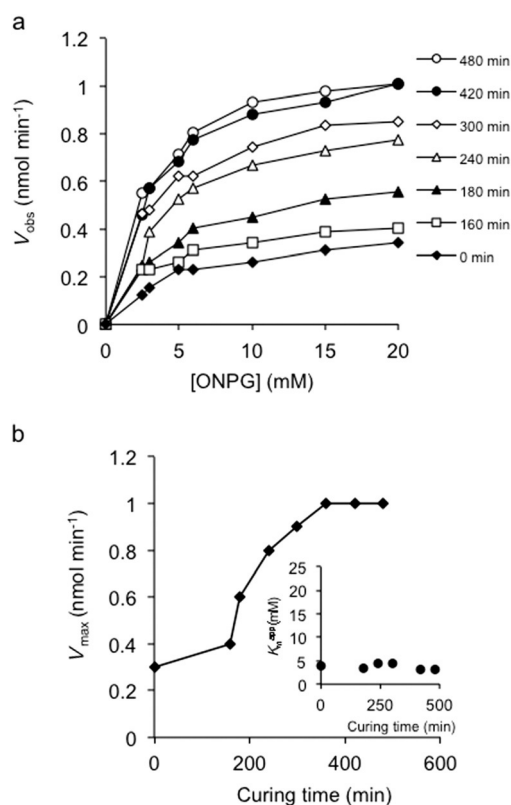


Figure 4. Recovery of enzymatic activity during the curing period. a) Reaction velocity of $\text{SNP}_{\text{ENZ-OS}}$ -catalyzed ONPG hydrolysis; the results for longer curing durations are similar to that observed after 480 min and are omitted for clarity of the figure. b) Apparent maximum velocity values ($V_{\text{m}}^{\text{app}}$) were extracted from the kinetic data by using a Lineweaver–Burk plot as a function of the curing time; the insert shows the evolution of the $K_{\text{m}}^{\text{app}}$ values measured for the same ONPG concentrations.

different; the biocatalytic activity increased to 118, 123, and 114% at 45, 50, and 55°C, respectively. Moreover, $\text{SNP}_{\text{ENZ-OS}}$ preserved 88% of its catalytic activity at 60°C. This gain in activity could be explained by a protective effect of the organosilica layer shielding the enzyme, along with an increase in the kinetic energy of the substrate molecules, thus resulting in an overall increase in the biocatalytic turnover rate.

To confirm this hypothesis and to gain further insight into the thermal stability of $\text{SNP}_{\text{ENZ-OS}}$, we incubated $\text{SNP}_{\text{ENZ-OS}}$ particles at 50°C for increasing durations of time and measured their biocatalytic activity at 40°C. Whereas both SNP_{ENZ} and β -gal lost more than 94 and 97% of their activity after incubation for only 10 and 20 min, respectively, the decay in the biocatalytic activity of $\text{SNP}_{\text{ENZ-OS}}$ was much slower, with only 25 and 40% activity loss after incubation for 10 and 20 min, respectively; more than 25% of the activity was preserved even after incubation for 60 min. To investigate further this thermal protective effect, we subjected $\text{SNP}_{\text{ENZ-OS}}$, SNP_{ENZ} , and β -gal to freezing–thawing cycles. The results showed that whereas SNP_{ENZ} and β -gal had already lost 45 and 25% of their activity, respectively, after the first cycle, the loss for $\text{SNP}_{\text{ENZ-OS}}$ was only 5%. Whereas both SNP_{ENZ} and β -

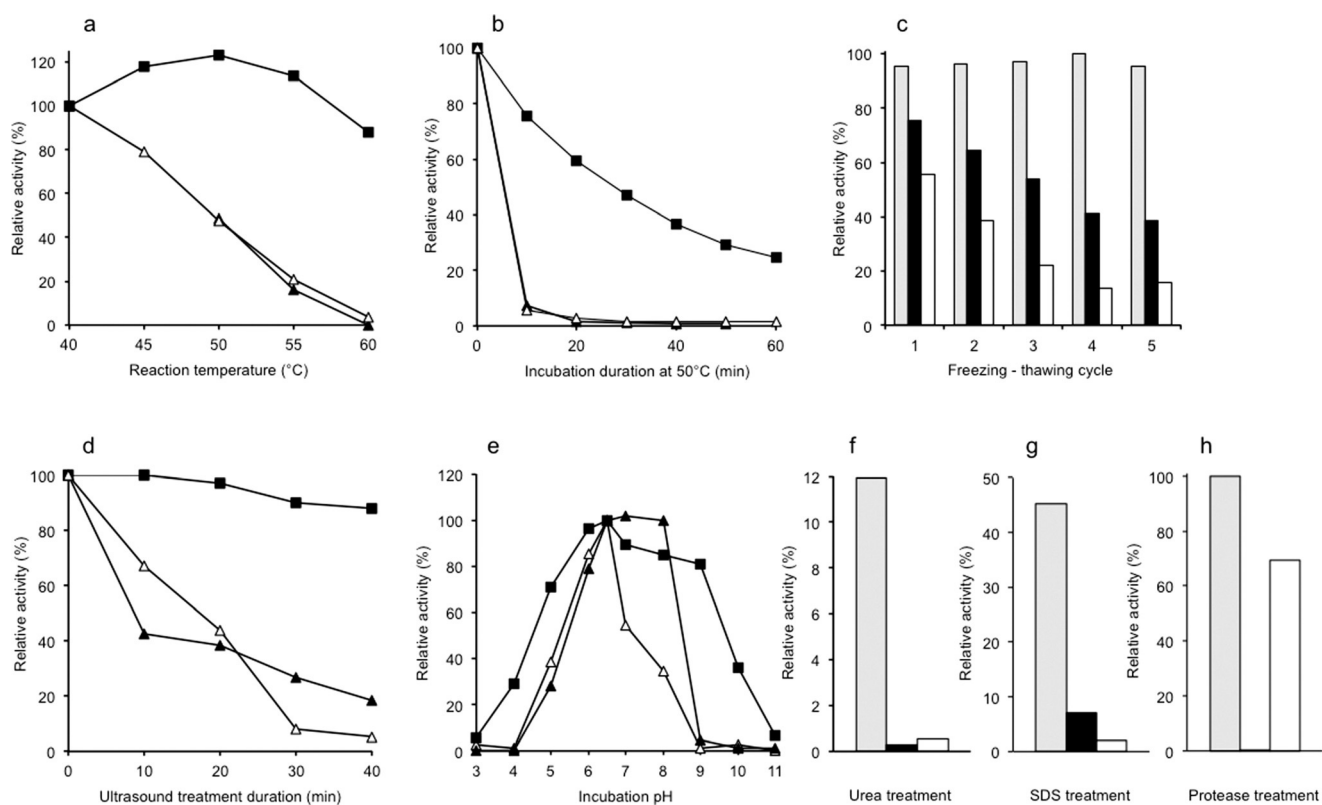


Figure 5. Physical, chaotropic, and biochemical stress tests. a) Relative activity of SNP_{ENZ-OS} (black squares), soluble β-gal (black triangles), and SNP_{ENZ} (white triangles) at different reaction temperatures. b) Relative activity of SNP_{ENZ-OS}, soluble β-gal, and SNP_{ENZ} after different incubation times at 50°C. c) Relative activity of SNP_{ENZ-OS} (gray bars), soluble β-gal (black bars), and SNP_{ENZ} (white bars) after different numbers of freeze–thaw cycles. d) Relative activity of SNP_{ENZ-OS}, soluble β-gal, and SNP_{ENZ} after different durations of ultrasound treatment. e) Relative activity of SNP_{ENZ-OS}, soluble β-gal, and SNP_{ENZ} after incubation in solutions with different pH values. f,g) Relative activity of SNP_{ENZ-OS}, soluble β-gal, and SNP_{ENZ} in the presence of 6 M urea (f) or 1% SDS (g). h) Relative activity of SNP_{ENZ-OS}, soluble β-gal, and SNP_{ENZ} after protease treatment for 1 h.

gal experienced a gradual loss of biocatalytic activity with each cycle to reach values of 15 and 38%, respectively, after 5 cycles, the biocatalytic activity of SNP_{ENZ-OS} remained relatively unchanged at 95%.

As an additional physical stress test, we subjected the particles to ultrasound. The particles were incubated in phosphate buffer in an ultrasonic bath at 25°C for increasing durations of time. Although the biocatalytic activity of both SNP_{ENZ} and β-gal decayed quite rapidly over time, the loss of activity of SNP_{ENZ-OS} was very moderate; SNP_{ENZ-OS} conserved 88% of its activity after 40 min (18% activity was conserved for β-gal and 5% for SNP_{ENZ}; Figure 5).

To assess the resistance of SNP_{ENZ-OS} to pH variation, we incubated the particles for 15 min at different pH values. For values lower than the optimum pH value of the enzyme (6.5), SNP_{ENZ} and β-gal showed a similar trend, with a loss of more than 40% activity at pH 5 and 100% at pH 4. By contrast, SNP_{ENZ-OS} was more stable and lost only 29 and 71% of its activity at the same pH values. When stored at pH 3, SNP_{ENZ-OS}, SNP_{ENZ}, and β-gal all lost more than 97% of their initial activity. As for pH values higher than the optimum value, SNP_{ENZ} lost more than 45 and 75% of activity at pH 7 and 8, respectively, whereas SNP_{ENZ-OS} lost only 10 and 15% activity. At these pH values, the most stable system is the soluble β-gal, which retained 100% activity. At pH 9 and 10,

SNP_{ENZ} and β-gal both lost more than 95% of their activity, whereas SNP_{ENZ-OS} lost only 19 and 64%, respectively. At higher pH values, the hydrolytic activity of SNP_{ENZ} and β-gal was reduced to 0%, whereas SNP_{ENZ-OS} retained 7% of its initial activity. Overall, these results clearly demonstrate that the organosilica layer had a beneficial effect on the resilience of the enzyme to pH changes.

We also studied the effect of the organosilica layer against chaotropic stress by using urea (6 M) and sodium dodecylsulfate (1%). The activity was measured directly under the denaturing conditions. In the presence of urea, neither SNP_{ENZ} nor β-gal exhibited any biocatalytic activity; however, 12% activity was measured for SNP_{ENZ-OS}. Urea acts as a potent H-bond donor and acceptor;^[11] it can also act as an enzyme inhibitor by forming H-bonds with important residues located in the active site of the enzyme. In the present case, one of the effects of the protective layer could be to preserve the active conformation of the protein; the loss in enzyme activity may be due in part to inhibition caused by the high concentration of urea.

In the case of SDS treatment, we showed that, as expected, the free β-gal was completely inactive under these conditions. Whereas the activity of SNP_{ENZ} was as low as 7%, SNP_{ENZ-OS} maintained 45% of its activity. The final assay that was performed was stability against protease digestion. As

Table 1: Immobilization and shielding of different enzymes.

| Enzyme | Enzyme size [nm ³] | Shell thickness [nm] | Specific activity ^[a] |
|----------------------------|--------------------------------|----------------------|----------------------------------|
| acid phosphatase | 4.0×6.0×7.5 | 12 | 23.0 ^[b] |
| laccase | 5.7×11.0×16.5 | 19 | 11.0 ^[c] |
| alcohol dehydrogenase | 10.5×10×5.5 | 13 | 1.5 ^[d] |
| aspartate aminotransferase | 10.5×6.3×5.4 | 18 | 75.0 ^[e] |

[a] Absolute activity (mU) per milligram of nanoparticles, measured using the substrate(s) indicated.

[b] Substrate: *p*-nitrophenyl phosphate. [c] Substrate: 2,2'-azinobis(3-ethylbenzothiazoline-6-sulfonic acid). [d] Substrate and cofactor: 2-amino-benzyl alcohol, NAD⁺. [e] Substrates: L-aspartate, 2-oxoglutarate.

expected, after incubation with proteinase K for 60 min, no activity was measured for β -gal, and a 30% loss of activity was measured for SNP_{ENZ}, thus suggesting that the accessibility of the immobilized enzyme partially hindered protease digestion. In the case of SNP_{ENZ-OS}, no loss of biocatalytic activity was measured, thus confirming that the shielded enzyme is not accessible to the protease.

To test the efficiency of the developed nanobiocatalysts in a real matrix, we tested the hydrolytic activity of the shielded β -galactosidase for its natural substrate, lactose, in skim milk by using ¹⁴C radioactively labeled lactose. The experimental results showed that the shielded enzyme catalyzed the conversion of lactose into glucose and galactose 30% more efficiently than soluble β -gal (see the Supporting Information).

To assess the versatility of the developed shielding strategy, we tested several different enzymes: acid phosphatase, laccase, alcohol dehydrogenase, aspartate aminotransferase (Table 1; see also the Supporting Information). For all tested enzymes, the shielding strategy turned out to be successful. More specifically, acid phosphatase, another hydrolase enzyme, was protected with an organosilica shell with a thickness of 12 nm, which was sufficient to cover the whole enzyme. The resulting nanobiocatalyst showed a relevant biocatalytic activity of 23 mU mg⁻¹. The activity of a shielded laccase, which is a copper-containing oxidase that requires oxygen as second substrate, demonstrated that the shielding organosilica layer does not prevent oxygen diffusion and that the protected enzyme is active after protection. In the case of a nicotinamide adenine dinucleotide (NAD⁺)-dependant alcohol dehydrogenase, the activity measured when the enzyme was fully shielded in the protective organosilica layer showed that this shell does not hinder the diffusion of the cofactor. Finally, the activity recovered for an aspartate aminotransferase demonstrated that the amine exchange between aspartic and oxoglutaric acids is not hampered in the protective organosilica shell.

In summary, we have developed a versatile strategy to produce nanobiocatalysts with enhanced stability. In these systems, a shielding organosilica layer makes the enzyme resistant to a large set of denaturing stresses.

Acknowledgements

Financial support from the Swiss Nanoscience Institute (SNI) through the NanoArgovia program (NanoZyme project), the Swiss Commission for Technology and Innovation (grant agreement 16437.1 PFEN-NM), the EU-Eurostars program (grant agreement E!6894), and the Swiss State Secretariat for Education, Research and Innovation (EU-H2020 INMARE project) is gratefully acknowledged.

Keywords: enzyme catalysis · nanobiocatalysts · nanoparticles · organosilica · self-assembly

How to cite: *Angew. Chem. Int. Ed.* **2016**, *55*, 6285–6289
Angew. Chem. **2016**, *128*, 6393–6397

- [1] P. Grunwald, *Industrial Biocatalysis*, CRC Press, Boca Raton, **2015**.
- [2] a) M. Goldsmith, D. S. Tawfik, *Methods Enzymol.* **2013**, *523*, 257–283; b) S. G. Peisajovich, D. S. Tawfik, *Nat. Methods* **2007**, *4*, 991–994.
- [3] a) U. Hanefeld, L. Gardossi, E. Magner, *Chem. Soc. Rev.* **2009**, *38*, 453–468; b) F. Secundo, *Chem. Soc. Rev.* **2013**, *42*, 6250–6261; c) U. T. Bornscheuer, *Angew. Chem. Int. Ed.* **2003**, *42*, 3336–3337; *Angew. Chem.* **2003**, *115*, 3458–3459.
- [4] a) M. Misson, H. Zhang, B. Jin, *J. R. Soc. Interface* **2015**, *12*, 20140891; b) L. Cao, *Carrier-bound Immobilized Enzymes: Principles, Applications and Design*, Wiley, Weinheim, **2006**.
- [5] K. Liang, R. Ricco, C. M. Doherty, M. J. Styles, S. Bell, N. Kirby, S. Mudie, D. Haylock, A. J. Hill, C. J. Doonan, P. Falcaro, *Nat. Commun.* **2015**, *6*, 7240.
- [6] D. P. Patterson, B. Schwarz, R. S. Waters, T. Gedeon, T. Douglas, *ACS Chem. Biol.* **2014**, *9*, 359–365.
- [7] a) C. Sanchez, P. Belleville, M. Popall, L. Nicole, *Chem. Soc. Rev.* **2011**, *40*, 696–753; b) R. Ciriminna, A. Fidalgo, V. Pandarus, F. Béland, L. M. Ilharco, M. Pagliaro, *Chem. Rev.* **2013**, *113*, 6592–6620; c) M. T. Reetz, A. Zonta, J. Sempelkamp, *Angew. Chem. Int. Ed. Engl.* **1995**, *34*, 301–303; *Angew. Chem.* **1995**, *107*, 373–376; d) M. T. Reetz, A. Zonta, J. Sempelkamp, *Biotechnol. Bioeng.* **1996**, *49*, 527–534.
- [8] a) E. Z. Eisenmesser, D. A. Bosco, M. Akke, D. Kern, *Science* **2002**, *295*, 1520–1523; b) K. A. Henzler-Wildman, M. Lei, V. Thai, S. J. Kerns, M. Karplus, D. Kern, *Nature* **2007**, *450*, 913–916.
- [9] a) A. Cumbo, B. Lorber, P. F. X. Corvini, W. Meier, P. Shahgaldian, *Nat. Commun.* **2013**, *4*, 1503; b) S. Sykora, A. Cumbo, G. Belliot, P. Pothier, C. Arnal, Y. Dudal, P. F. X. Corvini, P. Shahgaldian, *Chem. Commun.* **2015**, *51*, 2256–2258.
- [10] A. Pereira-Rodríguez, R. Fernández-Leiro, M. I. González-Siso, M. E. Cerdán, M. Becerra, J. Sanz-Aparicio, *J. Struct. Biol.* **2012**, *177*, 392–401.
- [11] J. Almarza, L. Rincon, A. Bahsas, F. Brito, *Biochemistry* **2009**, *48*, 7608–7613.

Received: January 19, 2016

Published online: April 9, 2016